Sox11-modified mesenchymal stem cells (MSCs) accelerate bone fracture healing: Sox11 regulates differentiation and migration of MSCs

Liangliang Xu,*[,†,1] Shuo Huang,*[,1] Yonghui Hou,[†,1] Yang Liu,* Ming Ni,* Fanbiao Meng,* Kuixing Wang,* Yunfeng Rui,* Xiaohua Jiang,[‡,§] and Gang Li*[,‡,§,¶,2]

*Department of Orthopaedics & Traumatology and [†]Stem Cell and Regeneration Theme, School of Biomedical Sciences and Li Ka Shing Institute of Health Sciences, The Chinese University of Hong Kong, Prince of Wales Hospital, Shatin, Hong Kong, People's Republic of China; [‡]Epithelial Cell Biology Research Center and [§]MOE Key Laboratory of Regenerative Medicine, School of Biomedical Sciences, The Chinese University of Hong Kong, Shatin, Hong Kong, People's Republic of China; and [¶]The CUHK-ACC Space Medicine Centre on Health Maintenance of Musculoskeletal System, Shenzhen Research Institute, The Chinese University of Hong Kong, Shenzhen, People's Republic of China

ABSTRACT   Mesenchymal stem cells (MSCs) are a promising cell resource for tissue engineering. Sry-related high-mobility group box 11 (Sox11) plays critical roles in neural development and organogenesis. In the present study, we investigated the role of Sox11 in regulating trilineage differentiation (osteogenesis, adipogenesis, and chondrogenesis) and migration of MSCs, and explored the effect of systemically administrated Sox11-modified MSCs on bone fracture healing using the rat model of open femur fracture. Our results demonstrated that Sox11 overexpression increased the trilineage differentiation and migration of MSCs, as well as cell viability under oxidative stress. The effect of Sox11 on osteogenesis was confirmed by ectopic bone formation assay conducted in nude mice. In addition, we found that Sox11 could activate the bone morphogenetic protein (BMP)/Smad signaling pathway in MSCs. By dual-luciferase reporter assay, we also demonstrated that Sox11 could transcriptionally activate runt-related transcription factor 2 (Runx2) and CXC chemokine receptor-4 (CXCR4) expression. The activation of the BMP/Smad signaling pathway and Runx2, CXCR4 expression may have a synergic effect, which largely contributed to the effect of Sox11 on MSC fate determination and migration. Finally, using an open femur fracture model in rats, we found that a larger number of MSCs stably expressing Sox11 migrated to the fracture site and improved bone fracture healing. Taken together, our study shows that Sox11 is an important regulator of MSC differentiation and migration, and Sox11-modified MSCs may have clinical implication for accelerating bone fracture healing, which can reduce the delayed unions or nonunions.—Xu, L., Huang, S., Hou, Y., Liu, Y., Ni, M., Meng,

BONE FRACTURES ARE VERY common, and >5% of the fractures are impaired, leading to nonunions and severe disabilities (1). The positive effect of mesenchymal stem cells (MSCs) on bone fracture healing has been reported previously (2). MSCs have a multipotent capacity to differentiate into a variety of cell types, including osteoblasts, adipocytes, chondrocytes, myoblasts, and neurons (3, 4). In response to stimuli, MSCs have the ability of homing to the target tissue. Also, MSCs have been shown to be immunosuppressive and anti-inflammatory; they do not express major histocompatibility complex (MHC)-II, CD80, CD86, and CD40, and minimally express MHC-I on the cell surface (3, 5, 6). These characteristics make MSCs a promising cell source for tissue engineering, particularly for bone regeneration. The capacities of differentiation and homing are 2 determinants for the clinical application of MSCs for bone regeneration. However, the capacity of MSCs to differentiate into functional osteoblasts remains limited for efficient bone regeneration (7), and the studies on MSCs homing are rather limited.

Sry-related high-mobility group (HMG) box 11 (Sox11) belongs to the Sox C group of Sox transcription factors. The Sox proteins are characterized by HMG box, which is a highly conserved DNA binding domain. The main

---

function of Sox11 is involved in neural development and organogenesis during fetal development (8, 9). It has been demonstrated that Sox11 was highly expressed in developing sensory neurons, and ablating Sox11 caused an arrest of axonal outgrowth *in vivo* and *in vitro* (10). The Sox11 knockout mice showed craniofacial and skeletal malformations, asplenia, and hypoplasia of the lung, stomach, and pancreas (11), implying that Sox11 may be associated with bone development. Recently, the role of Sox11 in MSCs has been studied. It has been identified as one of the MSC-characteristic transcription factors involved in MSC stemness regulation by DNA microarray analysis (12). Knocking down Sox11 in MSCs suppressed MSCs' self-renewal capacities and reduced their osteogenic and adipogenic differentiation potential. However, the exact role of Sox11 in MSC differentiation, migration, and the underlying mechanisms are still not clearly clarified.

MSC differentiation into mature functional osteoblasts is a complex process involving many transcriptional factors and signaling pathways, such as Wnt, runt-related transcription factor 2 (Runx2), bone morphogenetic proteins (BMPs), hedgehog, Osterix, *etc.* Runx2 is a master transcription factor for osteogenic differentiation, and mice with homozygous mutation in this gene showed a complete lack of ossification (13). BMPs, members of the TGF-β superfamily, are involved in many aspects of embryogenesis and homeostasis, such as neuronal development, osteogenesis, and bone remodeling (14–16). The significance of BMPs in development and osteogenesis has been reviewed (17). Studies in recent years have found that BMP signals are mediated by BMP receptors (type I and II), and Smad1, Smad5, and Smad8 are the immediate downstream factors, which play a central role in BMP signal transduction. Smad1, Smad5, and Smad8 are phosphorylated by the receptors and then form a complex with Smad4, and then the complex is translocated into the nucleus. In the nucleus, the phosphorylated Smads (pSmads) interact with the other transcription factors such as Runx2 to initiate transcription of genes.

The chemokine stromal cell–derived factor-1 (SDF1)/CXC chemokine receptor-4 (CXCR4) axis has been recognized to control the migration of MSCs (18, 19), and stimulating the expression of CXCR4 is one of the strategies for enhancing MSCs' migration capacity (20–22). In the mouse fracture model, it has been demonstrated that systemically injected MSCs could migrate to the bone fracture site, and the migration is mainly driven by the SDF1/CXCR4 signaling pathway (2).

In the present study, we demonstrated that Sox11 overexpression improved the trilineage differentiation and migration abilities of bone marrow (BM)-MSCs. The enhancing effect of Sox11 on osteogenesis was confirmed by ectopic bone formation assay conducted in nude mice. We found that the BMP/Smad signaling pathway was enhanced by Sox11 overexpression in MSCs. In addition, we also found that the promoter activity of Runx2 and CXCR4 was transcriptionally activated by Sox11. Finally, using an open femur fracture model, we have demonstrated that a larger number of MSCs stably expressing Sox11 migrated to the fracture site, initiated callus ossification, and improved bone fracture healing *in vivo*.

MATERIALS AND METHODS

Plasmid construction, transfection, production of lentivirus, and infection

To construct lentiviral vector expressing Sox11, the green fluorescent protein (GFP) gene in pLentiLox 3.7 (pLL3.7) was cut off by *Nhe*I and *Eco*RI and replaced by a linker that has multiple cloning sites. The sequence of the linker is as follows: 5′-GCTA-GCGCTACCGGTCGCCACCAGGCCTGCATGCTGATCAGGAT-CCCCCGGGTTTAAACGAATTC-3′.

The cDNA encoding GFP was cloned by PCR and reinserted into the reconstructed pLL3.7 at *Sma*I and *Eco*RI. The blasticidin selection gene was inserted into reconstructed pLL3.7 at *Bam*HI and *Sma*I to form fusion protein with GFP. To construct a bicistronic expression vector, the internal ribosome entry site (IRES) element was also inserted into the reconstructed pLL3.7 vector at *Sph*I and *Bam*HI; the final reconstructed pLL3.7 vector was named pLL3.7-MCS-IRES-Blasticidin/GFP. Finally, the gene encoding rat Sox11 (GenBank number NM_053349) was amplified and cloned into pLL3.7-MCS-IRES-Blasticidin/GFP vector by *in vitro* recombination.

Pseudolentiviruses were produced by transient transfection of 293FT packaging cells (Invitrogen, Carlsbad, CA, USA) using the calcium phosphate method. Culture supernatants were harvested at 48 and 72 h after transfection, and lentiviral particles were concentrated using PEG6000 (23). For transduction, 1×10^5 cells were seeded into a 6-well plate and incubated with lentiviruses and 8 μg/ml Polybrene in the incubator for 24 h. After 48 h, blasticidin (Invitrogen) was added into the medium to select MSCs stably expressing Sox11 (Sox11-MSCs) or empty vector (con-MSCs).

The promoter region of Runx2 (24) was cloned and ligated into pGL3 basic plasmid according to a previous study. The promoter sequence of rat CXCR4 was retrieved and analyzed against Ensembl genome databases (*http://www.ensembl.org*) and the UCSC Genome Bioinformatics browser (*http://genome.ucsc.edu*). The promoter region of CXCR4 that is 3000 bp upstream of the first exon was cloned using the PCR primers (forward 5′-GCGGTACCTCGCATACCTG-TAGTTCTAG-3′ and reverse 5′-TATCTCGAGCTCAGAGGG-TCACTGCTAC-3′) and ligated into pGL3 basic plasmid.

Cell culture

All experiments were approved by the Animal Research Ethics Committee of the authors' institutions. BM was flushed out from the bone cavity of the Sprague-Dawley rats and subjected to density gradient centrifugation over Lymphoprep (1.077 g/ml; Axis-Shield, Oslo, Norway) to obtain the mononuclear cells (MNCs). The MNCs were cultured in α-minimum essential medium (MEM), 10% fetal bovine serum (FBS), and 2 mM L-glutamine (Invitrogen) at 37°C with 5% CO_2. The cells were trypsinized and subjected to flow cytometry examination to confirm the MSCs' surface markers (CD90, CD44, CD73, CD31, and CD34).

Luciferase reporter gene assay

Luciferase assay was performed using the Dual-Luciferase Reporter Assay System (Promega, Madison, WI, USA) according to

---

(continued from previous page)
FBS, fetal bovine serum; GAPDH, glyceraldehyde-3-phosphate dehydrogenase; GFP, green fluorescent protein; H&E, hematoxylin and eosin; HMG, high-mobility group; IRES, internal ribosome entry site; MEM, minimum essential medium; MHC, major histocompatibility complex; MNC, mononuclear cell; MSC, mesenchymal stem cell; MTT, 3-(4,5-dimethylthiazol-2-yl)-2,5-diphenyltetrazolium bromide; OCN, osteocalcin; OIM, osteogenic induction medium; PPAR, peroxisome proliferator-activated receptor; pSmad, phosphorylated Smad; Runx2, runt-related transcription factor 2; SDF1, stromal cell-derived factor-1; Sox, Sry-related high-mobility group box; TBST, Tris-buffered saline with Tween 20; TV, total tissue volume

the manufacturer's instructions. 293T cells were cotransfected with 400 ng empty vector or pLL3.7-Sox11, pRunx2-luc, or pCXCR4-luc and 10 ng of the pRL-CMV using Lipofectamine 2000 (Life Technologies, Grand Island, NY, USA). The luciferase activity was measured at 48 h after transfection using FLUOstar Galaxy (BMG LABTECH, Ortenberg, Germany).

Osteogenic differentiation and alkaline phosphatase activity assay

The MSCs were trypsinized and replated in a 6-well plate at a concentration of 1×10^5 cells per well. These cells were incubated in the α-MEM for 2 or 3 d. The medium was then replaced by osteogenic induction medium (OIM) containing 100 nM dexamethasone, 10 mM β-glycerophosphate, and 0.05 mM L-ascorbic acid-2-phosphate. At 7 d after osteogenic induction, the alkaline phosphatase (ALP) activity assay was conducted using ALP-AMP (BioSystems, Barcelona, Spain), according to the manufacturer's instructions. The ALP activity was normalized to total protein concentration as measured by the Bradford method (Bio-Rad Laboratories, Hercules, CA, USA). The mineralization of MSCs was assessed by Alizarin Red S staining. Briefly, the cell/matrix layer was washed with PBS, fixed with 70% ethanol for 10 min, and stained with 0.5% Alizarin Red S (pH 4.1) (Sigma-Aldrich, St. Louis, MO, USA) for 5 min.

Adipogenic differentiation

The MSCs were trypsinized and replated in a 6-well plate at a concentration of 1×10^5 cells per well. These cells were incubated in the α-MEM for 2 or 3 d. The medium was then replaced by adipogenic induction medium (AIM) containing 10% FBS, 1 μM dexamethasone, 10 μg/ml insulin, 50 μM indomethacin, and 0.5 mM isobutyl-methylxanthine. Before staining, the cells were rinsed with PBS and fixed in 70% ethanol for 10 min. They were then incubated in 2% Oil Red O reagent for 5 min at room temperature, and excess stain was removed by washing with distilled water. The number of Oil Red O-positive adipocytes was counted. The experiment was repeated 3 times, 20 images were randomly taken, and about 1000 cells were counted in each experiment.

Chondrogenic differentiation

The MSCs were trypsinized and concentrated at 500 g for 10 min, and then the pelleted cells were incubated in a chemically defined chondrogenic induction medium consisting of high-glucose DMEM supplemented with 10 ng/ml recombinant human TGF-β1 (PeproTech, Rocky Hill, NJ, USA), 100 mM dexamethasone (Sigma-Aldrich), 1 mM sodium pyruvate, 0.2 mM ascorbic acid 2-phosphate (Sigma-Aldrich), and ITS+Premix (BD Biosciences, San Jose, CA, USA). The medium was changed every 3 d. The obtained cell pellets were prepared for paraffin sections. The deposition of glycosaminoglycans was assessed by Safranin O staining. The positive stain was viewed under a phase-contrast microscope (Leica Microsystems Wetzlar Gesellschaft mit beschränkter Haftung, Wetzlar, Germany).

Western blot

The cells were washed with cold PBS twice and harvested by scraping in cold cell extraction buffer (Invitrogen; catalog number FNN0011). Protein concentration was determined by the Bradford method (Bio-Rad Laboratories). Equal proteins were loaded onto 10% Tris/glycine gels for electrophoresis and then transferred to a PVDF membrane and blocked in 5% nonfat milk (Bio-Rad Laboratories) for 1 h at room temperature with rocking. The primary antibody, anti-pSmad1/pSmad5/pSmad8 (1:1000; Cell Signaling Technology, Danvers, MA, USA), anti-BMP2

(1:1000; Abcam, Cambridge, MA, USA), anti-BMPRIA (1:1000; Santa Cruz Biotechnology, Dallas, TX, USA), anti-Sox11 (1:1000; Santa Cruz Biotechnology), or anti–glyceraldehyde-3-phosphate dehydrogenase (GAPDH) (1:1000; Santa Cruz Biotechnology) then was added and incubated for 2 h at room temperature or at 4°C overnight. After washing in Tris-buffered saline with Tween 20 (TBST) 3 times (5 min for each time), the membrane was incubated with horseradish peroxidase-linked secondary antibodies (anti-mouse or anti-goat) for 1 h at room temperature. Following 3 TBST washes, protein was detected with the ECL blotting reagents (Amersham Biosciences, Piscataway, NJ, USA) according to the manufacturer's instructions. The band intensity was quantified using ImageJ software (NIH, Bethesda, MD, USA).

RNA extraction and real-time PCR

Total cellular RNA was isolated with RNeasy (Qiagen, Valencia, CA, USA) according to the manufacturer's instructions. First-strand cDNA was synthesized with Moloney murine leukemia virus reverse transcriptase (Promega). PCR amplification was performed using the ABI StepOne Plus System (Applied Biosystems, Foster City, CA, USA) with primer sets outlined in Supplemental Table 1. Primer sequences were determined through established GenBank sequences. β-Actin was used as an internal control to evaluate the relative expression.

MTT assay

The cell survival of MSCs was determined using MTT [3-(4,5-dimethylthiazol-2-yl)-2,5-diphenyltetrazolium bromide] assay. The con-MSCs and Sox11-MSCs were seeded at 2000 cells per well in a 96-well plate and incubated at 37°C, 5% CO_2, respectively. At d 3, these cells were challenged with 0–250 μM H_2O_2 for 24 h. The cells were then incubated in the α-MEM with MTT solution for 4 h at 37°C. The blue formazan crystals trapped in cells were dissolved in 100 μl DMSO. The absorbance at 550 nm then was measured with a plate reader.

Cell migration

Migration was assayed using BD Falcon (Bedford, MA, USA) cell culture insert, which is 8 μm in pore size. The upper chamber of the insert was plated with 0.5×10^5 Sox11-MSCs or con-MSCs in α-MEM. The lower chamber contained α-MEM supplemented with 10% FBS as chemoattractant. MSCs then were put into the incubator for 16 h. The MSCs remaining on the upper surface of the membrane were removed with a cotton swab. After being washed with PBS, the membrane was fixed with 4% paraformaldehyde for 15 min and stained with 0.5% crystal violet. The number of cells passed through the membrane was counted.

Ectopic bone formation

A total of 2×10^5 Sox11-MSCs or con-MSCs were loaded onto sterilized Skelite (Kingston, ON, Canada) resorbable bone graft substitute and incubated at 37°C for 3 h to allow them attach to the graft. There were 3 nude mice under general anesthesia, and the grafts with the cells then were implanted subcutaneously into the dorsal surfaces. The transplants were harvested 8 wk later and subjected to histologic examination. The sections were subjected to hematoxylin and eosin (H&E) staining as well as immunohistochemical staining of osteocalcin (OCN). The osteoid matrix areas were measured using ImageJ software; 5 microscopic fields were chosen from each sample and measured as reported previously (25).
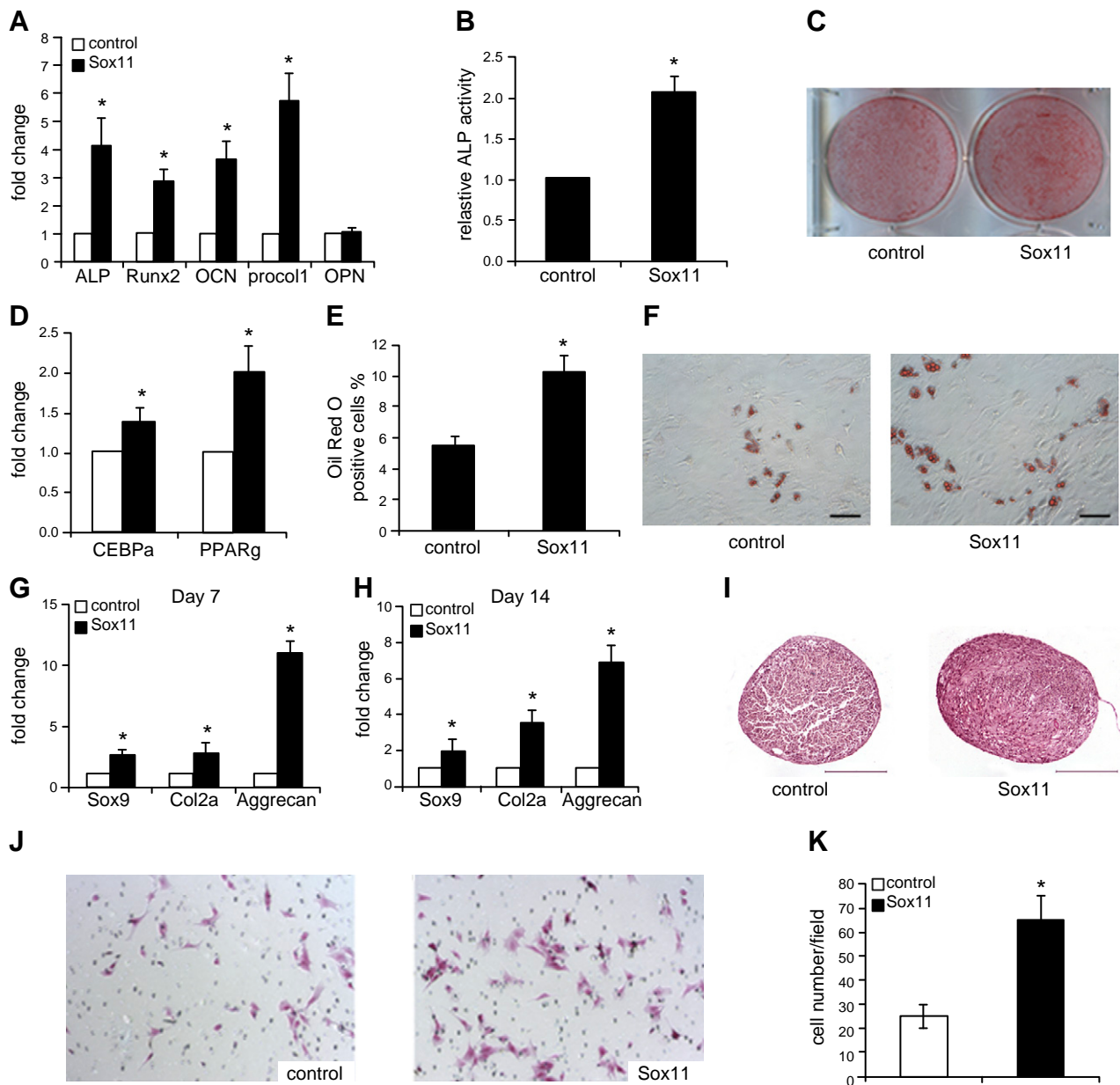
Figure 1. Sox11 promoted differentiation and migration of MSCs *in vitro*. BM-MSCs were transduced with lentivirus carrying Sox11 or empty vector, and then these MSCs were subjected to OIM, AIM, or CIM for several days. *A–C*) Sox11 promoted osteogenic differentiation of MSCs. *A*) After 7 d of osteogenic induction, the osteogenesis-related marker genes were analyzed by real-time PCR. *B*) The ALP activity of MSCs was measured after they were incubated with OIM for 7 d. *C*) Sox11 increased calcium deposition of MSCs. Alizarin Red staining is shown of MSCs after the cells were treated with OIM for 19 d. *D–F*) Sox11 promoted adipogenic differentiation of MSCs. *D, E*) After 14 d of adipogenic induction, the adipogenesis-related marker genes (CEBPα and PPARγ) were quantified with real-time PCR. The percentage of Oil Red O-positive cells in the 2 groups was calculated. *F*) Representative images of Oil Red O staining after the cells were treated with AIM for 14 d. *G–I*) Sox11 promoted chondrogenic differentiation of MSCs. *G, H*) MSCs were treated with CIM for 7 and 14 d, and then total RNA was extracted for real-time PCR analysis of chondrogenesis-related markers. *I*) Representative images of Safranin O staining of MSCs after the cells were treated with CIM for 21 d. *J, K*) Sox11 overexpression promoted migration of MSCs. The MSCs migrated through the membrane were detected with crystal violet staining. The number of MSCs was counted ($n = 3$). All the data represent the mean ± SD of 3 independent experiments. *$P < 0.05$. Scale bars, 100 μm.

Fracture healing model and analysis

Sprague-Dawley rats were anesthetized with ketamine and xylazine intraperitoneally. The open fracture model was established as previously reported (26). Sox11-MSCs or con-MSCs were injected into Sprague-Dawley rats through tail vein injection at 4 d after fracture ($n = 10$). The healing was monitored radiographically using a digital X-ray machine. Rats were killed at 7 and 35 d after cell injection. Femurs were harvested for micro-CT (computed tomography) analysis and then fixed in 4% buffered formalin, decalcified in 9% formic acid, and embedded in paraffin for sectioning. For micro-CT analysis, the femurs were scanned by vivaCT 40 (SCANCO Medical, Brüttisellen, Switzerland) using our previously established protocols (27). The

scan range covered 3 mm proximal and 3 mm distal to the fracture line with a resolution of 10.5 μm. Low- and high-density mineralized tissues were reconstructed using different thresholds (low attenuation, 160; high attenuation, 350) using our established evaluation protocol with small modification (28). The high-density tissues represented the newly formed highly mineralized calluses and the old cortices, whereas the low-density tissues represented the newly formed calluses. To assess the mechanical properties of the fractured femur, a mechanical test was performed as reported by our department (29). The sections were subjected to H&E or Safranin O staining or immunohistochemical staining of OCN as described previously (30). GFP-labeled MSCs were detected by immunohistochemical analysis using anti-GFP antibody (Santa Cruz Biotechnology). The number of GFP-positive cells was quantified by Image-Pro Plus 6.0 software (Media Cybernetics, Silver Spring, MD, USA) in 4 randomly selected sections from each sample of 3 different Sprague-Dawley rats. The region of interest was located near the fracture line.

Statistical analysis

All experiments were performed at least 3 times. All data were expressed as the mean $\pm$ sd. The data were analyzed by independent 2-tailed Student's t test using SPSS (version 16.0; Chicago, IL, USA). $P < 0.05$ was regarded as statistically significant.

RESULTS

Sox11 promoted trilineage differentiation and migration of BM-MSCs

To evaluate the effect of Sox11 on MSC differentiation and migration, the MSCs were transduced with lentivirus carrying Sox11 or empty vector, and then these MSCs were subjected to OIM, AIM, or chondrocyte induction medium (CIM) for several days, respectively. After 7 d of osteogenic induction, the osteogenesis-related marker genes were analyzed by real-time PCR analysis. The mRNA levels of ALP, OCN, collagen type I, and Runx2 were significantly up-regulated in MSCs overexpressing Sox11 (**Fig. 1**A). At the same time, we also measured the ALP activity and found that Sox11 overexpression significantly increased the ALP activity compared with the empty vector control cells (Fig. 1B). When the cells were treated with OIM for 19 d, more calcium deposits appeared in the MSC-overexpressing Sox11 group (Fig. 1C).

For adipogenesis, after 14 d of adipogenic induction, the adipogenesis-related marker genes [CCAAT/enhancer binding protein α (CEBPα) and peroxisome proliferator-activated receptor γ (PPARγ)] were quantified with real-time PCR; the results showed that both CEBPα and PPARγ were up-regulated by Sox11 overexpression (Fig. 1D). The percentage of Oil Red O-positive cells in Sox11-overexpressing MSCs was significantly higher than that of the control cells (Fig. 1E). Representative images of Oil Red O staining are shown in Fig. 1F.

For chondrogenesis, the MSCs were treated with CIM for 7 and 14 d before RNA extraction for real-time PCR analysis. The result demonstrated that Sox11 significantly up-regulated the chondrogenesis-related marker genes such as Sox9, aggrecan, and collagen type II α at both time points (Fig. 1G, H), meaning that Sox11 also promoted the chondrogenic differentiation of MSCs *in vitro*. After 21 d of
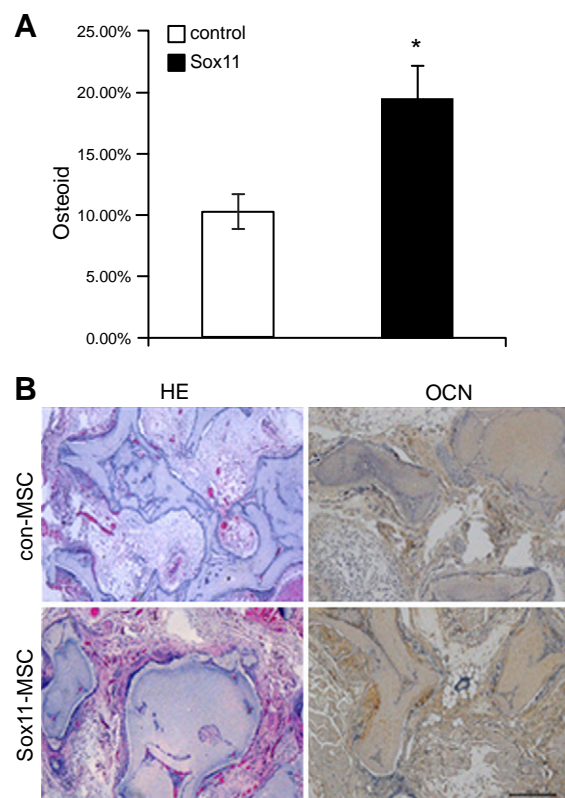

Figure 2. Overexpression of Sox11 in MSCs promoted ectopic bone formation *in vivo*. *A*) Sox11-MSCs and con-MSCs were loaded onto sterilized porous calcium phosphate restorable granules and implanted subcutaneously into the dorsal surfaces. The transplants were harvested 8 wk later for histologic examination. There were 5 microscopic fields from each sample used for quantification of new bone area ($n = 3$). *$P < 0.05$. *B*) Representative images of H&E staining and immunohistochemical staining of OCN. Amorphous osteoid matrix could be seen in the pores of transplants. Scale bar, 400 μm.

treatment with CIM, the cell pellets were fixed, sectioned, and stained with Safranin O. The staining result showed that Sox11-overexpressing MSCs had higher chondrogenic differentiation potential, compared to the control group (Fig. 1I).

In addition, we also checked the role of Sox11 in MSC migration because the migration ability is one of the most important characteristics of MSCs. The MSCs were transduced with lentivirus carrying Sox11 or empty vector control, an equal number of MSCs then were added into the upper layer of the BD Falcon cell culture insert, which is 8 μm in pore size. The lower chamber contained α-MEM supplemented with 10% FBS as chemoattractant. After incubation for 16 h, the number of MSCs that pass through the membrane was counted. Significantly more numbers of MSCs crossing the membrane were observed in the Sox11-overexpressing MSC group compared to the control MSC group (Fig. 1J, K).

Sox11 promoted ectopic bone formation of MSCs *in vivo*

In order to further confirm the effect of Sox11 on osteogenic differentiation of MSCs, Sox11-MSCs or con-MSCs

were loaded onto sterilized Skelite resorbable silicon-stabilized tricalcium phosphate bone graft substitutes and implanted s.c. at the dorsal sides. The transplants were harvested 8 wk later and subjected to histologic examination. The sections were subjected to H&E staining to observe the distribution of osteoid or immunohistochemical analysis to detect the expression of OCN. The histologic staining result suggested that the area of osteoid matrix in the Sox11-MSC group was about twice as much as that of the control MSC group (**Fig. 2***A*). The formation of bone-like tissue was confirmed by the presence of OCN and H&E staining of the osteoid (Fig. 2*B*).

Sox11 activated the BMP/Smad signaling pathway and CXCR4, Runx2 expression

Because the BMP/Smad signaling pathway is well known for its involvement in MSC differentiation and migration, we further asked whether Sox11 could activate the BMP/Smad signaling pathway in MSCs. Our real-time PCR result showed that Sox11 significantly increased the mRNA levels of BMP2, BMP4, BMPRI, and BMPRII (**Fig. 3***A*). In addition, we also detected the effect of Sox11 on the BMP/Smad signaling pathway by Western blot. The result

showed that Sox11 overexpression greatly increased the level of BMP2 and pSmad1/pSmad5/pSmad8 (Fig. 3*B*), suggesting that the BMP/Smad signaling pathway was enhanced by Sox11.

In Sox11-overexpressing MSCs, we found that the relative levels of trilineage differentiation and migration-related markers were significantly increased (Fig. 3*C*). Furthermore, we also found that Sox11 could bind with the CXCR4 or Runx2 promoter region and transcriptionally activate the expression of CXCR4 or Runx2, as demonstrated by dual-luciferase reporter assay (Fig. 3*D*, *E*). CXCR4 is an important regulator of cell migration, and Runx2 is a master transcription factor responsible for the osteogenesis of MSCs. Our results had indicated that the increased level of CXCR4, Runx2 as well as the enhanced BMP/Smad signaling pathway may be responsive in Sox11 promotion/enhancement of MSC differentiation and migration.

Sox11-modified MSCs accelerated bone fracture healing in an open femur fracture rat model

Finally, to determine whether Sox11 could accelerate bone fracture healing, open femur fractures were created in
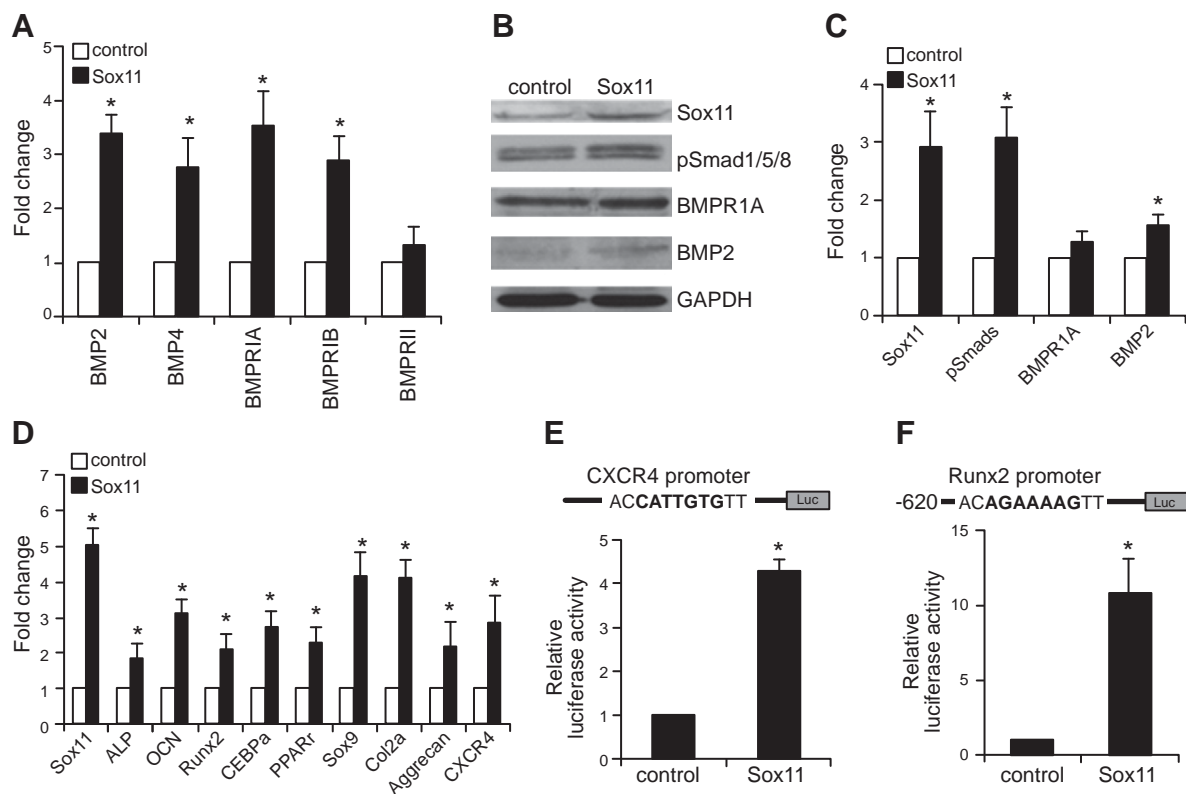

Figure 3. Sox11 activated the BMP/Smad signaling pathway and CXCR4, Runx2 expression. *A*) MSCs were transduced with lentivirus carrying Sox11 or empty vector, and then total RNA was extracted for real-time PCR to analyze the mRNA levels of BMP2, BMP4, BMPRIA/BMPRIB, and BMPRII. *B*) The effect of Sox11 on the BMP/Smad signaling pathway. The total proteins were extracted from MSCs transduced with Sox11 or control and then analyzed by Western blot using indicated antibodies. GAPDH was used as loading control. *C*) The relative levels of osteogenesis, adipogenesis, chondrogenesis, and migration-related marker genes were analyzed by real-time PCR in Sox11-overexpressing MSCs and control MSCs. *D*, *E*) Sox11 transcriptionally activated the expression of CXCR4 or Runx2. Luciferase activity assay was conducted in 293T cells as described in Materials and Methods. The putative Sox11 binding site is displayed in bold. The relative luciferase activity was quantified as normalized luciferase activity of control. All the data represent the mean ± SD of 3 independent experiments. *$P < 0.05$.

8-wk-old Sprague-Dawley rats. Sox11-MSCs or con-MSCs were injected systemically at 4 d after fracture. At 7 d after MSC injection, the calluses from rats that received Sox11-MSC injection showed larger areas of cartilage as demonstrated by H&E and Safranin O staining, indicating that the fracture repair in those rats proceeded through an endochondral ossification process much faster than those in the control groups (**Fig. 4A**). In addition, a great number of GFP-labeled MSCs were found homing to the site of fracture as shown by immunohistochemistry staining (Fig. 4A), and the number of GFP-labeled MSCs overexpressing Sox11 was greater than that of the control group (Fig. 4B). Our *in vitro* study showed that Sox11-MSCs exhibited a survival advantage over con-MSCs under the circumstance of oxidative stress, which could be one of the reasons accounting for more MSCs being observed in the fracture site apart from cell migration. As shown in Fig. 4C, Sox11-MSCs had higher cell survival capacity compared to con-MSCs when both of them were challenged by H_2O_2 at different concentrations for 24 h.

At 5 wk after MSC injection, the femurs were collected for micro-CT and histologic analysis. The results of micro-CT exhibited more bone formation in callus in the Sox11-MSC group compared with the control group (**Fig. 5A**). Quantitatively, the rats with Sox11-MSC injection displayed a significant increase in total bone volume (BV_t)/total tissue volume (TV) and volume of low-density bone (BV_l)/TV (Fig. 5B, C), whereas no differences were seen in the volume of high-density bone (BV_h)/TV (Fig. 5D and Supplemental Table 2), suggesting an enhanced bone formation process. To confirm functional recovery of the fractured bones, biomechanical evaluation by a 4-point bending test was performed. The result showed that the percentage ratios of mechanical properties (including ultimate load, energy to failure, and stiffness) in the fractured femur *vs.* the contralateral intact femur were significantly higher (except the stiffness) in the Sox11-MSC group than that of the control group (Fig. 5E–G).

In addition, the immunohistologic staining with GFP antibody showed that the GFP-labeled MSCs still localized in the fracture site, and a larger number of GFP-labeled MSCs displayed in the rats transplanted with Sox11-MSCs (**Fig. 6A**). Through defining the region of interest as illustrated in Fig. 6B, we calculated the relative area of bone and uncalcified region according to the histologic staining. The result showed that the percentage of bone in calluses of rats transplanted with Sox11-MSCs was higher than that of the control MSC group (Fig. 6C), as well as the percentage of cartilage in the uncalcified calluses (Fig. 6D).
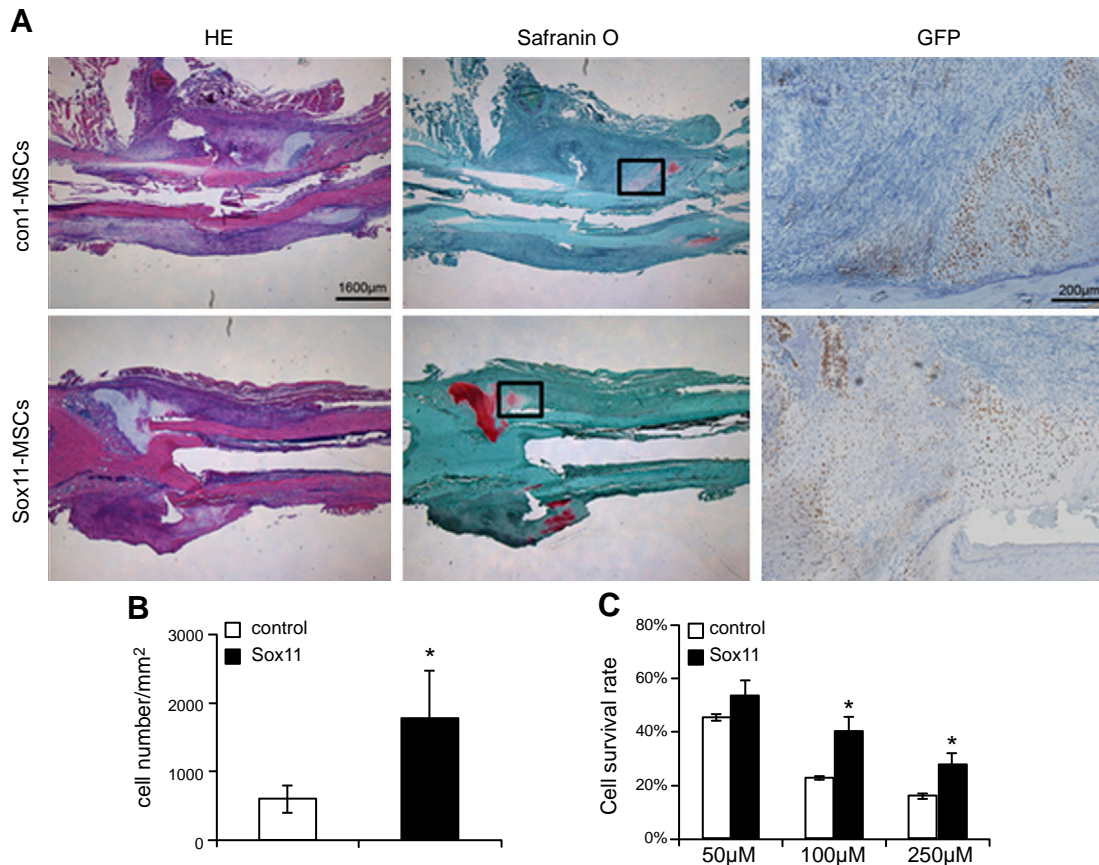

Figure 4. *A*) Sox11-modified MSCs increased the cartilaginous content of the calluses. At 1 wk after cell transplantation, the femurs were collected for histologic analysis. Longitudinal sections of calluses were subjected to H&E and Safranin O staining and immunohistochemical analysis using GFP antibody. *B*) The number of MSCs overexpressing Sox11 or empty vector was counted (*n* = 3). *C*) Sox11-modified MSCs exhibited survival advantage over control MSCs when the cells were treated with H_2O_2 *in vitro*. The MSCs were treated with indicated concentrations of H_2O_2 for 24 h, and then the cell viability was measured by MTT assay. *P < 0.05.
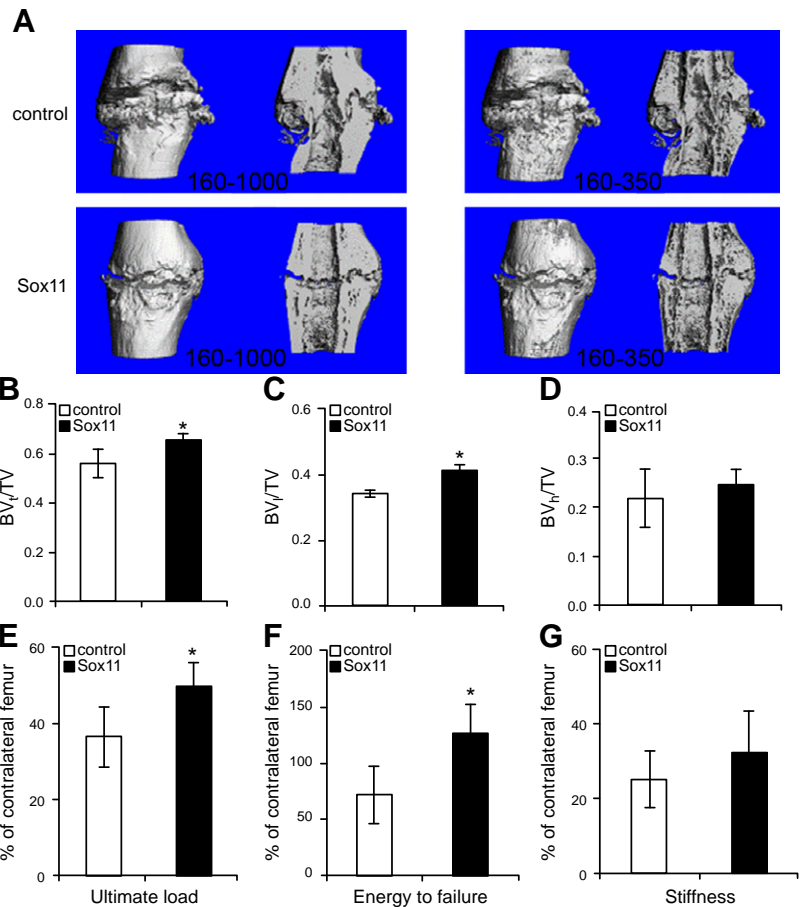
Figure 5. Micro-CT and mechanical test analysis of fracture calluses. At 5 wk after cell transplantation, the femurs were collected for micro-CT analysis. *A*) Representative 3-dimensional images and 2-dimensional sections generated from micro-CT analysis of femur fracture healing in rats transplanted with Sox11-MSCs and control-MSCs. Attenuation >160 represented total mineralized tissue, and attenuation between 160 and 350 represented the newly formed calluses. *B–D*) The bone volume densities (BV_t/TV, BV_l/TV, and BV_h/TV) were analyzed by micro-CT ($n = 4$). *E–G*) Mechanical properties of the fractured bones by 4-point bending test. The mechanical properties (including ultimate load, energy to failure, and stiffness) in the fractured femur were normalized with contralateral intact femur (in percentage; $n = 5$). $*P < 0.05$.

DISCUSSION

In the present study, we found that Sox11 promoted trilineage differentiation and migration of MSCs, and systemic administration of allogenic Sox11-modified MSCs could accelerate bone fracture healing using Sprague-Dawley rat models. Therefore, our study provides important clues for the development of new therapeutic strategies in bone regeneration.

Sox11 has been reported to be involved in neural development and organogenesis during fetal development (8, 9). The Sox11 knockout mice showed craniofacial and skeletal malformations (11). It has been identified as one of the MSC-characteristic transcription factors involved in MSC stemness regulation (12). In this study, we have demonstrated that Sox11-overexpressing MSCs showed enhanced trilineage differentiation and migration abilities. These interesting findings further lead us to ask whether Sox11 could activate the BMP/Smad signaling pathway in MSCs because it is well known for its involvement in regulating MSC differentiation and migration. Kang *et al.* (31) have conducted a comprehensive analysis of 14 types of BMPs for their abilities to regulate the multilineage-specific differentiation of MSCs. They found that BMP 2, 4, 5, 7, and 9 effectively induced both osteogenic and adipogenic differentiation *in vitro* and *in vivo*. In our study, the *in vitro* result clearly showed that Sox11 could activate the BMP/Smad signaling pathway in MSCs, which partially contributes to the enhanced trilineage differentiation and migration abilities of MSCs. In addition, we also

found that Sox11 could transcriptionally activate the expression of CXCR4 and Runx2. CXCR4, a specific receptor for SDF1, plays essential roles in hematopoiesis and organogenesis (32, 33). Mice lacking CXCR4 die *in utero* and are defective in vascular development, hematopoiesis, and cardiogenesis (34). Recently, the SDF1/CXCR4 axis has been recognized to control the migration of MSCs (18, 19). CXCR4 genetically modified MSCs have been used for postinfarction myocardial repair in rats through intravenous delivery, and the results suggested that the number of MSCs homing toward the infracted myocardium was markedly increased, thereby leading to improved cardiac performance (22). Runx2, a transcription factor that belongs to the Runx family, has been well known to be an essential master transcription factor for osteoblast differentiation. *Runx2*-deficient mice showed a complete lack of ossification (13). Runx2 has been shown to act in synergy with BMP-induced osteogenic differentiation (31). Thus, the effect of Sox11 on MSC differentiation and migration may be mediated by the BMP/Smad signaling pathway synergizing with Runx2, CXCR4, and other effectors such as Sox9, PPARγ, *etc.*

In addition, we also checked the effect of Sox11 on the osteogenesis of MSCs using an *in vivo* ectopic bone formation model. The result showed that increased osteoid formation was observed in Sox11-overexpressing MSCs when the MSCs combined with grafts were transplanted in nude mice. Furthermore, in order to determine whether Sox11-overexpressing MSCs could be used to accelerate bone fracture healing, we used an open femur fracture
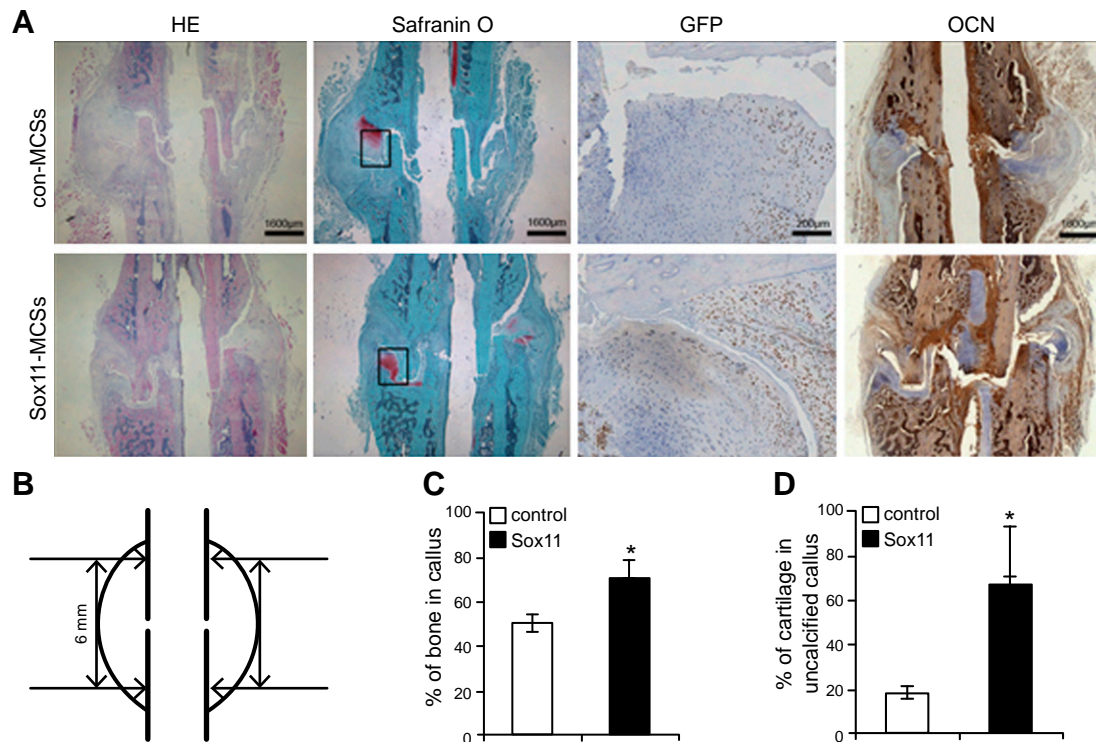
Figure 6. Histologic analysis of fracture calluses. At 5 wk after cell transplantation, the femurs were collected for histologic analysis. *A*) Longitudinal sections of calluses were subjected to H&E and Safranin O staining and immunohistochemical analysis with GFP and OCN antibodies. *B*) The region of interest was 3 mm below and above the fracture line identified in the sections. *C, D*) The percentage of bone in callus and chondrocytes in the uncalcified callus was calculated using ImageJ software according to histologic staining. Sections were obtained from at least 4 rats from each group. *$P < 0.05$.

model created in 8-wk-old Sprague-Dawley rats. The result demonstrated that a larger number of Sox11-overexpressing MSCs migrated to the fracture site and accelerated the fracture repair process. The results of micro-CT quantitatively exhibited a greater bone volume density in the Sox11-MSC group compared with that of the control group in the fracture callus. The biomechanical evaluation indicated that the percentage ratios of mechanical properties in the fractured femur *vs.* the contralateral intact femur were higher in the Sox11-MSC group than that of the control group. The number of MSCs is an important determinant influencing the effect of MSCs on fracture healing. It has been pointed out that the effect of transplanted MSCs on fracture repair is dependent on the number of cells presented at the fracture site (35). Our *in vitro* result demonstrated that Sox11 could promote cell migration by increasing CXCR4 as well as cell viability under oxidative stress, which would contribute to the higher number of MSCs in the fracture callus. In addition, according to the histologic staining, we found that the percentage of bone in calluses of rats transplanted with Sox11-MSCs was higher than that of the control MSC group, as well as the percentage of cartilage in the uncalcified calluses. These data demonstrated that systemic administration of Sox11-overexpressing MSCs could accelerate bone fracture healing. In a stabilized tibia fracture mouse model, the systemically transplanted mouse MSCs have been shown to migrate to the fracture site and improve the fracture healing (2). This report and our results provide evidence that systemically transplanted MSCs or genetically modified MSCs are applicable and effective for promoting bone fracture repair.

In summary, we demonstrated that Sox11 could enhance the trilineage differentiation and migration of BM-MSCs. We found that the BMP/Smad signaling pathway was enhanced by Sox11 overexpression in MSCs. In addition, we also found that the promoter activity of Runx2 and CXCR4 was activated by Sox11. In an open femur fracture model, we have demonstrated that MSCs stably expressing Sox11 migrated to the fracture site, initiated callus ossification, and improved bone fracture healing. These findings suggest that Sox11 plays important roles in regulating osteogenic differentiation and migration of MSCs. Our findings support that using genetically modified Sox11-MSCs to enhance fracture repair may be a potential new MSC-based therapy. FJ

REFERENCES

1. Victoria, G., Petrisor, B., Drew, B., and Dick, D. (2009) Bone stimulation for fracture healing: what's all the fuss? *Indian J. Orthop.* **43**, 117–120

2. Granero-Moltó, F., Weis, J. A., Miga, M. I., Landis, B., Myers, T. J., O'Rear, L., Longobardi, L., Jansen, E. D., Mortlock, D. P., and Spagnoli, A. (2009) Regenerative effects of transplanted mesenchymal stem cells in fracture healing. *Stem Cells* **27**, 1887–1898

3. Pittenger, M. F., Mackay, A. M., Beck, S. C., Jaiswal, R. K., Douglas, R., Mosca, J. D., Moorman, M. A., Simonetti, D. W., Craig, S., and Marshak, D. R. (1999) Multilineage potential of adult human mesenchymal stem cells. *Science* **284**, 143–147

4. Jiang, Y., Jahagirdar, B. N., Reinhardt, R. L., Schwartz, R. E., Keene, C. D., Ortiz-Gonzalez, X. R., Reyes, M., Lenvik, T., Lund, T., Blackstad, M., Du, J. B., Aldrich, S., Lisberg, A., Low, W. C., Largaespada, D. A., and Verfaillie, C. M. (2002) Pluripotency of mesenchymal stem cells derived from adult marrow. *Nature* **418**, 41–49

5. Deans, R. J., and Moseley, A. B. (2000) Mesenchymal stem cells: biology and potential clinical uses. *Exp. Hematol.* **28**, 875–884

6. Tse, W. T., Beyer, W., Pendleton, J. D., D'Andrea, A., and Guinan, E. C. (2000) Bone marrow-derived mesenchymal stem cells suppress T cell activation without inducing allogeneic anergy. *Blood* **96**, 241a

7. Petite, H., Viateau, V., Bensaïd, W., Meunier, A., de Pollak, C., Bourguignon, M., Oudina, K., Sedel, L., and Guillemin, G. (2000) Tissue-engineered bone regeneration. *Nat. Biotechnol.* **18**, 959–963

8. Kuhlbrodt, K., Herbarth, B., Sock, E., Enderich, J., Hermans-Borgmeyer, I., and Wegner, M. (1998) Cooperative function of POU proteins and SOX proteins in glial cells. *J. Biol. Chem.* **273**, 16050–16057

9. Azuma, T., Ao, S., Saito, Y., Yano, K., Seki, N., Wakao, H., Masuho, Y., and Muramatsu, M. (1999) Human SOX11, an upregulated gene during the neural differentiation, has a long 3′ untranslated region. *DNA Res.* **6**, 357–360

10. Lin, L., Lee, V. M., Wang, Y., Lin, J. S., Sock, E., Wegner, M., and Lei, L. (2011) Sox11 regulates survival and axonal growth of embryonic sensory neurons. *Dev. Dyn.* **240**, 52–64

11. Sock, E., Rettig, S. D., Enderich, J., Bösl, M. R., Tamm, E. R., and Wegner, M. (2004) Gene targeting reveals a widespread role for the high-mobility-group transcription factor Sox11 in tissue remodeling. *Mol. Cell. Biol.* **24**, 6635–6644

12. Kubo, H., Shimizu, M., Taya, Y., Kawamoto, T., Michida, M., Kaneko, E., Igarashi, A., Nishimura, M., Segoshi, K., Shimazu, Y., Tsuji, K., Aoba, T., and Kato, Y. (2009) Identification of mesenchymal stem cell (MSC)-transcription factors by microarray and knockdown analyses, and signature molecule-marked MSC in bone marrow by immunohistochemistry. *Genes Cells* **14**, 407–424

13. Komori, T., Yagi, H., Nomura, S., Yamaguchi, A., Sasaki, K., Deguchi, K., Shimizu, Y., Bronson, R. T., Gao, Y. H., Inada, M., Sato, M., Okamoto, R., Kitamura, Y., Yoshiki, S., and Kishimoto, T. (1997) Targeted disruption of Cbfa1 results in a complete lack of bone formation owing to maturational arrest of osteoblasts. *Cell* **89**, 755–764

14. Yoon, B. S., and Lyons, K. M. (2004) Multiple functions of BMPs in chondrogenesis. *J. Cell. Biochem.* **93**, 93–103

15. Wan, M., and Cao, X. (2005) BMP signaling in skeletal development. *Biochem. Biophys. Res. Commun.* **328**, 651–657

16. Wu, X., Shi, W., and Cao, X. (2007) Multiplicity of BMP signaling in skeletal development. *Ann. N. Y. Acad. Sci.* **1116**, 29–49

17. Chen, D., Zhao, M., and Mundy, G. R. (2004) Bone morphogenetic proteins. *Growth Factors* **22**, 233–241

18. Wynn, R. F., Hart, C. A., Corradi-Perini, C., O'Neill, L., Evans, C. A., Wraith, J. E., Fairbairn, L. J., and Bellantuono, I. (2004) A small proportion of mesenchymal stem cells strongly expresses functionally active CXCR4 receptor capable of promoting migration to bone marrow. *Blood* **104**, 2643–2645

19. Li, Y., Yu, X., Lin, S., Li, X., Zhang, S., and Song, Y. H. (2007) Insulin-like growth factor 1 enhances the migratory capacity of mesenchymal stem cells. *Biochem. Biophys. Res. Commun.* **356**, 780–784

20. Shi, M., Li, J., Liao, L., Chen, B., Li, B., Chen, L., Jia, H., and Zhao, R. C. (2007) Regulation of CXCR4 expression in human mesenchymal stem cells by cytokine treatment: role in homing efficiency in NOD/SCID mice. *Haematologica* **92**, 897–904

21. Tsai, L. K., Leng, Y., Wang, Z., Leeds, P., and Chuang, D. M. (2010) The mood stabilizers valproic acid and lithium enhance mesenchymal stem cell migration via distinct mechanisms. *Neuropsychopharmacology* **35**, 2225–2237

22. Cheng, Z., Ou, L., Zhou, X., Li, F., Jia, X., Zhang, Y., Liu, X., Li, Y., Ward, C. A., Melo, L. G., and Kong, D. (2008) Targeted migration of mesenchymal stem cells modified with CXCR4 gene to infarcted myocardium improves cardiac performance. *Mol. Ther.* **16**, 571–579

23. Kutner, R. H., Zhang, X. Y., and Reiser, J. (2009) Production, concentration and titration of pseudotyped HIV-1-based lentiviral vectors. *Nat. Protoc.* **4**, 495–505

24. Drissi, H., Luc, Q., Shakoori, R., Chuva De Sousa Lopes, S., Choi, J. Y., Terry, A., Hu, M., Jones, S., Neil, J. C., Lian, J. B., Stein, J. L., Van Wijnen, A. J., and Stein, G. S. (2000) Transcriptional autoregulation of the bone related CBFA1/RUNX2 gene. *J. Cell. Physiol.* **184**, 341–350

25. Liu, Y., Wang, L., Kikuiri, T., Akiyama, K., Chen, C., Xu, X., Yang, R., Chen, W., Wang, S., and Shi, S. (2011) Mesenchymal stem cell-based tissue regeneration is governed by recipient T lymphocytes via IFN-γ and TNF-α. *Nat. Med.* **17**, 1594–1601

26. Tägil, M., McDonald, M. M., Morse, A., Peacock, L., Mikulec, K., Amanat, N., Godfrey, C., and Little, D. G. (2010) Intermittent PTH(1-34) does not increase union rates in open rat femoral fractures and exhibits attenuated anabolic effects compared to closed fractures. *Bone* **46**, 852–859

27. He, Y. X., Liu, Z., Pan, X. H., Tang, T., Guo, B. S., Zheng, L. Z., Xie, X. H., Wang, X. L., Lee, K. M., Li, G., Cao, Y. P., Wei, L., Chen, Y., Yang, Z. J., Hung, L. K., Qin, L., and Zhang, G. (2012) Deletion of estrogen receptor beta accelerates early stage of bone healing in a mouse osteotomy model. *Osteoporos. Int.* **23**, 377–389

28. Hao, Y. J., Zhang, G., Wang, Y. S., Qin, L., Hung, W. Y., Leung, K., and Pei, F. X. (2007) Changes of microstructure and mineralized tissue in the middle and late phase of osteoporotic fracture healing in rats. *Bone* **41**, 631–638

29. Shi, H. F., Cheung, W. H., Qin, L., Leung, A. H. C., and Leung, K. S. (2010) Low-magnitude high-frequency vibration treatment augments fracture healing in ovariectomy-induced osteoporotic bone. *Bone* **46**, 1299–1305

30. Tran, D., Golick, M., Rabinovitz, H., Rivlin, D., Elgart, G., and Nordlow, B. (2000) Hematoxylin and safranin O staining of frozen sections. *Dermatol. Surg.* **26**, 197–199

31. Kang, Q., Song, W. X., Luo, Q., Tang, N., Luo, J., Luo, X., Chen, J., Bi, Y., He, B. C., Park, J. K., Jiang, W., Tang, Y., Huang, J. Y., Su, Y. X., Zhu, G. H., He, Y., Yin, H., Hu, Z. M., Wang, Y., Chen, L., Zuo, G. W., Pan, X. C., Shen, J. K., Vokes, T., Reid, R. R., Haydon, R. C., Luu, H. H., and He, T. C. (2009) A comprehensive analysis of the dual roles of BMPs in regulating adipogenic and osteogenic differentiation of mesenchymal progenitor cells. *Stem Cells Dev.* **18**, 545–559

32. Nagasawa, T. (2000) A chemokine, SDF-1/PBSF, and its receptor, CXC chemokine receptor 4, as mediators of hematopoiesis. *Int. J. Hematol.* **72**, 408–411

33. Ratajczak, M. Z., Zuba-Surma, E., Kucia, M., Reca, R., Wojakowski, W., and Ratajczak, J. (2006) The pleiotropic effects of the SDF-1-CXCR4 axis in organogenesis, regeneration and tumorigenesis. *Leukemia* **20**, 1915–1924

34. Tachibana, K., Hirota, S., Iizasa, H., Yoshida, H., Kawabata, K., Kataoka, Y., Kitamura, Y., Matsushima, K., Yoshida, N., Nishikawa, S., Kishimoto, T., and Nagasawa, T. (1998) The chemokine receptor CXCR4 is essential for vascularization of the gastrointestinal tract. *Nature* **393**, 591–594

35. Bruder, S. P., Fink, D. J., and Caplan, A. I. (1994) Mesenchymal stem cells in bone development, bone repair, and skeletal regeneration therapy. *J. Cell. Biochem.* **56**, 283–294